Activation of C_2H_6 and C_3H_8 by Gas-Phase Mo^+: Thermochemistry of Mo−Ligand Complexes

P. B. Armentrout*

Department of Chemistry, University of Utah, Salt Lake City, Utah 84112

Received June 12, 2007

The kinetic energy dependences of the reactions of Mo^+ (^6S) with ethane and propane have been studied using guided ion beam mass spectrometry. No exothermic reactions are observed in these systems, in contrast to results for the neighboring element, Nb^+. At slightly elevated energies, dehydrogenation of the two hydrocarbons is observed as the dominant process at low energies in both reaction systems. At high energies, products resulting from both C−H and C−C cleavage processes are appreciable. Modeling of the endothermic reaction cross-sections yields the 0 K bond dissociation energies (in eV) of $D_0(Mo-H) = 2.06 \pm 0.19$, $D_0(Mo^+-H_2) = 0.14 \pm 0.15$, $D_0(Mo^+-CH) = 5.32 \pm 0.14$, $D_0(Mo^+-CH_3) = 1.57 \pm 0.09$, $D_0(Mo^+-C_2H) = 3.25 \pm 0.22$, $D_0(Mo^+-C_2H_2) \geq 1.87 \pm 0.05$, $D_0(Mo^+-C_2H_3) = 2.95 \pm 0.15$, $D_0(Mo^+-C_2H_4) \geq 0.82 \pm 0.03$, $D_0(Mo^+-C_2H_5) = 2.09 \pm 0.14$, $D_0(Mo^+-C_3H_2) = 4.34 \pm 0.21$, $D_0(Mo^+-C_3H_4) = 2.22 \pm 0.03$, and $D_0(Mo^+-C_3H_6) \geq 0.81 \pm 0.05$. The ionization energy of MoH is also derived as 7.43 ± 0.20 eV. The results for Mo^+ are compared to those for the first-row transition-metal congener, Cr^+, and the neighboring element, Nb^+.

Introduction

In 1988, Schilling and Beauchamp asked "What Is Wrong with Gas-Phase Chromium? A Comparison of the Unreactive Chromium (1+) Cation with the Alkane-Activating Molybdenum Cation".[1] This provocative title was the result of their observations that Mo^+ reacts with all alkanes, except methane, to give dehydrogenation products, whereas Cr^+ does not. This work was performed using an ion beam experiment at low kinetic energies of about 0.25 eV. Somewhat later, using ion cyclotron resonance (ICR) mass spectrometry, Cassady and McElvany[2] found that neither ethane nor propane reacted with Mo^+ at thermal energies, although larger hydrocarbons did react, albeit inefficiently. They attributed the difference in observations to the likelihood that these reactions are actually thermoneutral or slightly endothermic, rather than being exothermic. In the present work, we revisit these systems to more quantitatively characterize the reactivity of Mo^+ over a wide range of kinetic energies. This permits the extraction of systematic thermodynamic and mechanistic information, as well as providing insight into just how reactive molybdenum cations really are.

This study augments a long-term research goal in our laboratory to study the reactions of transition-metal ions (M^+) with small hydrocarbons. Such studies have revealed the electronic requirements for the activation of C−H and C−C bonds at metal centers[3−6] and provide an examination of the periodic trends in such reactivity unavailable in condensed-phase media.[3,7] A particular strength of the guided ion beam methods used in our laboratory is the derivation of metal−hydrogen and metal−carbon bond dissociation energies (BDEs).[8−12] Such thermochemistry is of obvious fundamental interest and also has implications for understanding a variety of catalytic reactions involving transition-metal systems.[13] Studies of such systems for first-row transition-metal elements are extensive,[3−12] and those for second-row transition-metal cations are also abundant[1,2,14−25] but less systematic.[26] In our laboratory, we have studied the activation of several small hydrocarbons by the

* Corresponding author. Fax: (801) 581-8433; e-mail: armentrout@chem.utah.edu.

(1) Schilling, J. B.; Beauchamp, J. L. *Organometallics* **1988**, *7*, 194.
(2) Cassady, C. J.; McElvany, S. W. *Organometallics* **1992**, *11*, 2367.
(3) For reviews, see: Armentrout, P. B. In *Selective Hydrocarbon Activation: Principles and Progress*; Davies, J. A., Watson, P. L., Greenberg, A., Liebman, J. F., Eds.; Wiley VCH: New York, 1990; p 467. Armentrout, P. B. In *Gas Phase Inorganic Chemistry*; Russell, D. H., Ed.; Plenum: New York, 1989; p 1. Armentrout, P. B.; Beauchamp, J. L. *Acc. Chem. Res.* **1989**, *22*, 315.
(4) Armentrout, P. B. *Science* **1991**, *251*, 175. Armentrout, P. B. *Annu. Rev. Phys. Chem.* **1990**, *41*, 313.
(5) Weisshaar, J. C. *Adv. Chem. Phys.* **1992**, *82*, 213. Weisshaar, J. C. *Acc. Chem. Res.* **1993**, *26*, 213.
(6) van Koppen, P. A. M.; Kemper, P. R.; Bowers, M. T. *J. Am. Chem. Soc.* **1992**, *114*, 1083. van Koppen, P. A. M.; Kemper, P. R.; Bowers, M. T. In *Organometallic Ion Chemistry*; Freiser, B. S., Ed.; Kluwer: Dordrecht, The Netherlands, 1995; pp 157−196.
(7) Allison, J. *Prog. Inorg. Chem.* **1986**, *34*, 627. Squires, R. R. *Chem. Rev.* **1987**, *87*, 623. Russell D. H. *Gas Phase Inorganic Chemistry*; Plenum: New York, 1989. Eller, K.; Schwarz, H. *Chem. Rev.* **1991**, *91*, 1121.
(8) Armentrout, P. B.; Georgiadis, R. *Polyhedron* **1988**, *7*, 1573.
(9) Armentrout, P. B. *ACS Symp. Ser.* **1990**, *428*, 18.
(10) Armentrout, P. B.; Clemmer, D. E. In *Energetics of Organometallic Species*; Simoes, J. A. M., Beauchamp, J. L., Eds.; Kluwer: Dordrecht, The Netherlands, 1992; p 321.
(11) Armentrout, P. B.; Kickel, B. L. In *Organometallic Ion Chemistry*; Freiser, B. S., Ed.; Kluwer: Dordrecht, The Netherlands, 1995; pp 1−45.
(12) Freiser, B. S. *Organometallic Ion Chemistry*; Kluwer: Dordrecht, The Netherlands, 1995.
(13) Crabtree, R. H. *Chem. Rev.* **1985**, *85*, 245.
(14) Byrd, G. D.; Freiser, B. S. *J. Am. Chem. Soc.* **1982**, *104*, 5944.
(15) Huang, Y.; Wise, M. B.; Jacobson, D. B.; Freiser, B. S. *Organometallics* **1987**, *6*, 346.
(16) Buckner, S. W.; MacMahon, T. J.; Byrd, G. D.; Freiser, B. S. *Inorg. Chem.* **1989**, *28*, 3511.
(17) Buckner, S. W.; Freiser, B. S. *J. Am. Chem. Soc.* **1987**, *109*, 1247.
(18) Gord, J. R.; Freiser, B. S.; Buckner, S. W. *J. Chem. Phys.* **1989**, *91*, 7530.
(19) Ranasinghe, Y. A.; MacMahon, T. J.; Freiser, B. S. *J. Phys. Chem.* **1991**, *95*, 7721.
(20) Mandich, M. L.; Halle, L. F.; Beauchamp, J. L. *J. Am. Chem. Soc.* **1984**, *106*, 4403.
(21) Tolbert, M. A.; Mandich, M. L.; Halle, L. F.; Beauchamp, J. L. *J. Am. Chem. Soc.* **1986**, *108*, 5675.
(22) Tolbert, M. A.; Beauchamp, J. L. *J. Phys. Chem.* **1986**, *90*, 5015.
(23) Kickel, B. L.; Armentrout, P. B. *J. Am. Chem. Soc.* **1995**, *117*, 4057.

10.1021/om700579m CCC: $37.00
Publication on Web 10/11/2007

Table 1. Mo^+-L Bond Energies (eV) at 0 K

	this work		previous work	
species	expt	theory[a]	expt	theory
Mo^+-H		1.62−2.02	1.72 (0.06)[b]	1.35,[c] 1.53 (0.13),[d] 1.79,[e] 1.91[f]
Mo−H	2.06 (0.19)	2.33−2.48	>1.85, <2.15,[g] >2.1, <2.5[h]	2.13,[i] 2.19[j]
Mo^+-H_2	0.14 (0.15)	0.25−0.31		∼0.2[e]
Mo^+-C		3.96−4.34	4.31 (0.20),[k] 4.55 (0.19)[l]	
Mo^+-CH	5.32 (0.14)	4.74−4.92	5.12 (0.30)[l]	
Mo^+-CH_2		2.96−3.44	3.57 (0.10)[l]	3.08 (0.17)[m]
Mo^+-CH_3	1.57 (0.09)	1.70−1.89	1.63 (0.12)[l]	1.38 (0.13),[i] 1.31[n]
Mo^+-2CH_3		3.80		2.93 [3.45][o]
Mo^+-C_2H	3.25 (0.22)	3.57−3.64		
$Mo^+-C_2H_2$	≥1.87 (0.05)	1.47−1.59		0.85 (0.13)[p]
$Mo^+-C_2H_3$	2.95 (0.15)	2.16−2.50		
$HMo^+-C_2H_2$	2.69 (0.17)	1.92−2.36		
$H-Mo^+(C_2H_2)$	2.54 (0.16)	2.34−2.38		
$Mo^+-C_2H_4$	≥0.82 (0.03)	1.26−1.39		
$Mo^+-C_2H_5$	2.09 (0.14)	2.09−2.37		
$Mo^+-C_2H_6$		0.59		0.39[o]
$Mo^+-C_3H_2$	4.34 (0.21)			
$Mo^+-C_3H_4$	2.22 (0.03)			
$Mo^+-C_3H_6$	>0.81 (0.05)	1.41		

[a] Range shown corresponds to high and low values determined at several different levels of theory: see Table S1 and ref 36. Single values were determined at the B3LYP/HW/6-311++G(3df,3p) level. [b] Ref 37. [c] Ref 68. [d] Best estimate value including corrections for errors in the computed atomic splittings (0.09 eV) and basis set incompleteness (0.04 eV) from ref 69. [e] Ref 43. [f] Ref 70. [g] Ref 39. [h] Schilling and Beauchamp as reported in ref 22. [i] Ref 41. [j] Ref 42. [k] Ref 38. [l] Ref 36. [m] Ref 72. [n] Ref 73. [o] Ref 45. Value in brackets is empirically adjusted. [p] Ref 44.

second-row transition-metal ions: Y^+,[27] Zr^+,[28,29] Nb^+,[30] Ru^+,[31] Rh^+,[32,33] Pd^+,[34] and Ag^+.[35] Thus, molybdenum is the only second-row transition-metal cation (other than technetium) not subjected to this rigorous treatment. Recently, we reported results for reactions of Mo^+ with methane,[36] and here, we extend this work by examining the reactions of Mo^+ with ethane and propane.

There is relatively little thermochemistry available for molybdenum species in the literature, as shown in Table 1. We have previously measured BDEs for Mo^+-H, Mo^+-O, and Mo^+-CH_x ($x = 0-3$) by determining the endothermicities of the formation of these species from reactions of Mo^+ with H_2 (and D_2),[37] CO,[38] and CH_4 (and CD_4).[36] This latter work discusses all relevant experimental and theoretical studies in the literature for MoH^+ and $MoCH_x^+$ ($x = 0-3$). For species unique to the present study, the only other experimental studies of relevance are for neutral Mo−H, where the bond energy has been measured by Sallans et al.[39] and Tolbert and Beauchamp, as reported in ref 22. In addition, theoretical calculations have been performed for MoH,[40−42] $Mo(H)_2^+$,[43] $Mo^+(C_2H_2)$,[44] $Mo(CH_3)_2^+$, and $Mo^+(C_2H_6)$.[45]

Experimental and Theoretical Procedures

General. These studies were performed using a guided ion beam tandem mass spectrometer. The instrument and experimental methods have been described previously.[46,47] Ions, formed as described next, are extracted from the source, accelerated, and focused into a magnetic sector momentum analyzer for mass analysis. In these studies, $^{98}Mo^+$, the heaviest stable isotope, was used throughout. The ions were decelerated to a desired kinetic energy and focused into an octopole ion guide that radially trapped the ions. While in the octopole, the ions passed through a gas cell that contained the neutral reactant at pressures (<0.2 mTorr) where multiple collisions are improbable (<7% at 0.5 eV). Explicit examination of the pressure dependence of the cross-sections measured here verifies that the results shown are the result of single collisions only. The product and remaining reactant ions drifted out of the gas cell, were focused into a quadrupole mass filter, and then were detected by a secondary electron scintillation detector. Ion intensities were converted to absolute cross-sections as described previously.[46] Uncertainties in the absolute cross-sections were estimated at ±20%.

To determine the absolute zero and distribution of the ion kinetic energy, the octopole was used as a retarding energy analyzer.[46] The uncertainty in the absolute energy scale was ±0.05 eV (lab). The full width at half-maximum (fwhm) of the ion energy distribution was 0.2−0.4 eV (lab). Lab energies were converted into center-of-mass energies using $E(\mathrm{CM}) = E(\mathrm{lab})\, m/(m + M)$,

(24) Blomberg, M. R. A.; Siegbahn, P. E. M.; Svensson, M. *J. Phys. Chem.* **1994**, *98*, 2062.
(25) Blomberg, M. R. A.; Siegbahn, P. E. M.; Svensson, M.; Wennerberg, J. J. In *Energetics of Organometallic Species*; Martinho Simoes, J. A., Ed.; Kluwer: Dordrecht, The Netherlands, 1992; pp 387−421.
(26) Armentrout, P. B. Organometallic bonding and reactivity. In *Topics in Organometallic Chemistry*; Brown, J. M., Hofmann, P., Eds.; Springer-Verlag: Berlin, 1999; Vol. 4, pp 1−45.
(27) Sunderlin, L. S.; Armentrout, P. B. *J. Am. Chem. Soc.* **1989**, *111*, 3845.
(28) Armentrout, P. B.; Sievers, M. R. *J. Phys. Chem. A* **2003**, *107*, 4396.
(29) Sievers, M. R.; Armentrout, P. B. *Organometallics* **2003**, *22*, 2599−2611.
(30) Sievers, M. R.; Chen, Y.-M.; Haynes, C. L.; Armentrout, P. B. *Int. J. Mass Spectrom.* **2000**, *195*−*196*, 149.
(31) Armentrout, P. B.; Chen, Y.-M. *J. Am. Soc. Mass Spectrom.* **1999**, *10*, 821−839.
(32) Chen, Y.-M.; Armentrout, P. B. *J. Phys. Chem.* **1995**, *99*, 10775.
(33) Chen, Y.-M.; Armentrout, P. B. *J. Am. Chem. Soc.* **1995**, *117*, 9291.
(34) Chen, Y.-M.; Sievers, M. R.; Armentrout, P. B. *Int. J. Mass Spectrom. Ion Processes* **1997**, *167*−*168*, 195.
(35) Chen, Y.-M.; Armentrout, P. B. *J. Phys. Chem.* **1995**, *99*, 11424.
(36) Armentrout, P. B. *J. Phys. Chem. A* **2006**, *110*, 8327−8338.
(37) Sievers, M. R.; Chen, Y.-M.; Elkind, J. L.; Armentrout, P. B. *J. Phys. Chem.* **1996**, *100*, 54.
(38) Sievers, M. R.; Chen, Y.-M.; Armentrout, P. B. *J. Chem. Phys.* **1996**, *105*, 6322.
(39) Sallans, L.; Lane, K. R.; Squires, R. R.; Freiser, B. S. *J. Am. Chem. Soc.* **1985**, *107*, 4379−4385.
(40) Langhoff, S. R.; Pettersson, L. G. M.; Bauschlicher, C. W., Jr. *J. Chem. Phys.* **1987**, *86*, 268.
(41) Bauschlicher, C. W., Jr.; Langhoff, S. R.; Partridge, H.; Barnes, L. A. *J. Chem. Phys.* **1989**, *91*, 2399.
(42) Balasubramanian, K. *J. Chem. Phys.* **1990**, *93*, 8061.
(43) Das, K. K.; Balasubramanian, K. *J. Chem. Phys.* **1989**, *91*, 6254.
(44) Sodupe, M.; Bauschlicher, C. W., Jr. *J. Phys. Chem.* **1991**, *95*, 8640.
(45) Rosi, M.; Bauschlicher, C. W., Jr.; Langhoff, S. R.; Partridge, H. *J. Phys. Chem.* **1990**, *94*, 8656.
(46) Ervin, K. M.; Armentrout, P. B. *J. Chem. Phys.* **1985**, *83*, 166.
(47) Schultz, R. H.; Armentrout, P. B. *Int. J. Mass Spectrom. Ion Processes* **1991**, *107*, 29.

where M and m are the masses of the ion and neutral reactant, respectively. At the lowest energies, the ion energies were corrected for truncation of the ion beam as described previously.[46] All energies stated next are in the center-of-mass frame.

Ion Source. The ion source used here was a dc discharge/flow tube (DC/FT) source described in previous work.[47] The DC/FT source utilized a molybdenum cathode held at 1.5−3 kV over which a flow of approximately 90% He and 10% Ar passed at a typical pressure of ~0.5 Torr. Ar^+ ions created in a direct current discharge were accelerated toward the molybdenum cathode, sputtering off atomic metal ions. The ions then underwent $\sim 10^5$ collisions with He and $\sim 10^4$ collisions with Ar in the meter long flow tube before entering the guided ion beam apparatus. Results obtained previously[37] indicate that the Mo^+ ions produced in the DC/FT source are exclusively in their ^6S ground state (<0.1% excited states).

Data Analysis. Previous theoretical[48,49] and experimental work[50] has shown that endothermic cross-sections can be modeled by using eq 1

$$\sigma(E) = \sigma_0 \Sigma g_i (E + E_{el} + E_i - E_0)^n / E \quad (1)$$

where σ_0 is an energy independent scaling parameter, E is the relative translational energy of the reactants, E_{el} is the average electronic energy of the Mo^+ reactant (0.0 eV here), E_0 is the reaction threshold at 0 K, and n is a parameter that controls the shape of the cross-section. The summation is over each rovibrational state of the reactants having relative populations g_i and energies E_i. The vibrational frequencies used in this work are taken from the literature.[51]

Before comparison with the data, the model was convoluted over the neutral and ion kinetic energy distributions using previously developed methods.[46] The parameters E_0, σ_0, and n were then optimized using a nonlinear least-squares analysis to best reproduce the data. Reported values of E_0, σ_0, and n were mean values for each parameter taken from the best fits to several independent sets of data. Uncertainties were one standard deviation from the mean. The listed uncertainties in the E_0 values also included the uncertainty in the absolute energy scale.

Theoretical Approach. Most quantum chemistry calculations performed here were computed with the B3LYP hybrid density functional method[52−54] using the Gaussian 03 suite of programs.[55] Because the transition states of interest here often involve bridging hydrogens, the rather large 6-311++G(3df,3p) basis set is used for carbon and hydrogen. This basis set gives good results for the thermochemistry of ethane and dihydrogen, with deviations from experiment of less than 0.25 eV for the BDEs (theory vs experiment taken from ref 34 of $H-C_2H_5$ (4.191 vs 4.314 eV), $H_2-C_2H_4$ (1.276 vs 1.339 eV), $H-C_2H_3$ (4.629 vs 4.757 eV), $H_2-C_2H_2$ (1.777 vs 1.739 eV), $H-C_2H$ (5.724 vs 5.688 eV), CH_3-CH_3 (3.572 vs 3.813 eV), and H−H (4.508 vs 4.478 eV). The basis set on molybdenum was the Hay−Wadt (n + 1) ECP VDZ (HW),[56] equivalent to the Los Alamos ECP (LANL2DZ) basis set, in which 28 core electrons were described by a relativistic effective core potential (ECP).[57] We also tested the addition of the *f*-polarization functions described by Frenking and co-workers for the Hay−Wadt ECP (HW*)[58] for comparison with experimental thermochemistry. In all cases, the thermochemistry reported here was corrected for zero point energy (ZPE) effects (with frequencies scaled by 0.989).[59]

In our recent study of the reactions of Mo^+ with methane,[36] the thermochemistry of MoH^+ and $MoCH_x^+$ (x = 0−3) was carefully examined at several levels of theory: B3LYP, Becke Half and Half LYP (BHLYP),[60,61] MP2(full),[62] and QCISD(T)[63] approaches using the HW, HW*, and Stuttgart−Dresden (SD) ECP basis set.[64] Mean absolute deviations (MADs) between experimental and theoretical BDEs for these five molybdenum species using the HW* basis were 0.31, 0.90, 0.53, and 0.26 eV for the B3LYP, BHLYP, MP2, and QCISD(T) approaches, respectively, such that the best agreement between experiment and theory was achieved with the B3LYP and QCISD(T) approaches, with the latter giving slightly better agreement. The HW* and SD basis sets for molybdenum gave comparable results, which were slightly better than those for the HW basis (by about 0.08 eV). For the more complicated species examined in this work, we limited our calculations to B3LYP and QCISD(T) approaches using both HW and HW* basis sets. The QCISD(T) single point calculations utilize geometries and ZPE calculated at the B3LYP level.

For many of the species examined here, calculations of excited states were obtained by explicitly moving electrons into other orbitals to create states of alternate configuration and/or symmetry. Optimizations of the geometry were then carried out in the usual way. In all cases, these calculations were conducted at the B3LYP/HW/6-311++G(3df,3p) level.

Results

Cross-sections for reaction of Mo^+ with the two small alkanes are presented in the following sections. In some cases, these cross-sections have been corrected for mass overlap between product ions having adjacent masses. Thermodynamic information for the stable and radical hydrocarbons required to interpret these results has been compiled.[34] The only additional values

(48) Aristov, N.; Armentrout, P. B. *J. Am. Chem. Soc.* **1986**, *108*, 1806.
(49) Chesnavich, W. J.; Bowers, M. T. *J. Phys. Chem.* **1979**, *83*, 900.
(50) Armentrout, P. B. In *Advances in Gas Phase Ion Chemistry*; Adams, N. G., Babcock, L. M., Eds.; JAI: Greenwich, 1992; Vol. 1, pp 83−119.
(51) Shimanouchi, T. *Table of Molecular Vibrational Frequencies, Consolidated*; National Bureau of Standards: Washington, DC, 1972; Vol. 1.
(52) Becke, A. D. *J. Chem. Phys.* **1993**, *98*, 5648.
(53) Lee, C.; Yang, W.; Parr, R. G. *Phys. Rev. B* **1988**, *37*, 785.
(54) Stephens, P. J.; Devlin, F. J.; Chabalowski, C. F.; Frisch, M. J. *J. Phys. Chem.* **1994**, *98*, 11623.
(55) Frisch, M. J.; Trucks, G. W.; Schlegel, H. B.; Scuseria, G. E.; Robb, M. A.; Cheeseman, J. R.; Montgomery, J. A., Jr.; Vreven, T.; Kudin, K. N.; Burant, J. C.; Millam, J. M.; Iyengar, S. S.; Tomasi, J.; Barone, V.; Mennucci, B.; Cossi, M.; Scalmani, G.; Rega, N.; Petersson, G. A.; Nakatsuji, H.; Hada, M.; Ehara, M.; Toyota, K.; Fukuda, R.; Hasegawa, J.; Ishida, M.; Nakajima, T.; Honda, Y.; Kitao, O.; Nakai, H.; Klene, M.; Li, X.; Knox, J. E.; Hratchian, H. P.; Cross, J. B.; Bakken, V.; Adamo, C.; Jaramillo, J.; Gomperts, R.; Stratmann, R. E.; Yazyev, O.; Austin, A. J.; Cammi, R.; Pomelli, C.; Ochterski, J. W.; Ayala, P. Y.; Morokuma, K.; Voth, G. A.; Salvador, P.; Dannenberg, J. J.; Zakrzewski, V. G.; Dapprich, S.; Daniels, A. D.; Strain, M. C.; Farkas, O.; Malick, D. K.; Rabuck, A. D.; Raghavachari, K.; Foresman, J. B.; Ortiz, J. V.; Cui, Q.; Baboul, A. G.; Clifford, S.; Cioslowski, J.; Stefanov, B. B.; Liu, G.; Liashenko, A.; Piskorz, P.; Komaromi, I.; Martin, R. L.; Fox, D. J.; Keith, T.; Al-Laham, M. A.; Peng, C. Y.; Nanayakkara, A.; Challacombe, M.; Gill, P. M. W.; Johnson, B.; Chen, W.; Wong, M. W.; Gonzalez, C.; Pople, J. A. *Gaussian 03*, revision B.02; Gaussian, Inc.: Pittsburgh, PA, 2004.
(56) Hay, P. J.; Wadt, W. R. *J. Chem. Phys.* **1995**, *82*, 299.
(57) Basis sets used for Mo were obtained from the Extensible Computational Chemistry Environment Basis Set Database, Version 10/29/02, as developed and distributed by the Molecular Science Computing Facility, Environmental and Molecular Sciences Laboratory, which is part of the Pacific Northwest Laboratory and funded by the U.S. Department of Energy. The Pacific Northwest Laboratory is a multi-program laboratory operated by Battelle Memorial Institute for the U.S. Department of Energy under Contract DE-AC06-76RLO 1830.
(58) Ehlers, A. W.; Böhme, M.; Dapprich, S.; Boggi, A.; Höllwarth, A.; Jonas, V.; Köhler, K. F.; Stegmann, R.; Veldkamp, A.; Frenking, G. *Chem. Phys. Lett.* **1993**, *208*, 111.
(59) Foresman, J. B.; Frisch, M. J. *Exploring Chemistry with Electronic Structure Methods*, 2nd ed.; Gaussian, Inc.: Pittsburgh, PA, 1996.
(60) Holthausen, M. C.; Heinemann, C.; Cornehl, H. H.; Koch, W.; Schwarz, H. *J. Chem. Phys.* **1995**, *102*, 4931.
(61) Holthausen, M. C.; Mohr, M.; Koch, W. *Chem. Phys. Lett.* **1995**, *240*, 245.
(62) Møller, C.; Plesset, M. S. *Phys. Rev.* **1934**, *46*, 618.
(63) Pople, J. A.; Head-Gordon, M.; Raghavachari, K. *J. Chem. Phys.* **1987**, *87*, 5968.
(64) Andrae, D.; Haeussermann, U.; Dolg, M.; Stoll, H.; Preuss, H. *Theor. Chim. Acta* **1990**, *77*, 123.

needed here are the heats of formation at 0 K for C_2H, 5.82 ± 0.03 eV,[65] and C_3H_2, 5.61 ± 0.17 eV.[66]

$Mo^+ + C_2H_6$. The reaction of the molybdenum cation with ethane yields the products listed in reactions 2−11. These are shown in Figure 1a for products in which the CC bond remains intact and in Figure 1b for products that cleave the CC bond.

$$Mo^+ + C_2H_6 \rightarrow MoH^+ + C_2H_5 \quad (2)$$

$$\rightarrow MoH_2^+ + C_2H_4 \quad (3)$$

$$\rightarrow MoC^+ + H_2 + (CH_3 + H) \quad (4)$$

$$\rightarrow MoCH^+ + CH_3 + H_2 \quad (5)$$

$$\rightarrow MoCH_2^+ + (CH_3 + H) \quad (6)$$

$$\rightarrow MoCH_3^+ + CH_3 \quad (7)$$

$$\rightarrow MoC_2H^+ + 2H_2 + H \quad (8)$$

$$\rightarrow MoC_2H_2^+ + 2H_2 \quad (9)$$

$$\rightarrow MoC_2H_3^+ + H_2 + H \quad (10)$$

$$\rightarrow MoC_2H_4^+ + H_2 \quad (11)$$

At the lowest energies in our study (~0.08 eV), we found a cross-section for reaction 11 near the limits of our ability to detect ions, $\sigma(MoC_2H_4^+) = 8 \pm 2 \times 10^{-20}$ cm^2. When this cross-section was converted to a rate constant, we obtained 5.7 ± 1.4 × 10^{-15} cm^3/s, a result consistent with the observations of Cassady and McElvany who placed an upper limit for thermal reactions of 10^{-13} cm^3/s.[2] In contrast, Schilling and Beauchamp,[1] who created ground state Mo^+ using surface ionization, report both reactions 9 and 11 with a branching ratio of 17:83 at a center-of-mass energy of approximately 0.25 eV and a total cross-section of 4 × 10^{-17} cm^2. At 0.25 eV, our results yield a cross-section for reaction 11 of 2.0 ± 0.4 × 10^{-18} cm^2, and the cross-section for reaction 9 is within the experimental noise of about 1 × 10^{-19} cm^2. We do not find a branching ratio comparable to that observed by Schilling and Beauchamp until about 1.5 eV. The reason for the discrepancy can probably be attributed to two factors: (1) the limited ability of the Caltech ion beam apparatus, which does not incorporate an octopole ion beam guide, to accurately approach low energies and (2) the use of higher pressures of ethane (1−1.5 mTorr vs 0.2 mTorr used here), which could stabilize intermediates and products by secondary collisions, although the shorter reaction length in the Caltech instrument should mediate this factor. Some indication for the latter factor is the observation of Mo^+(alkane) adducts in the studies of Schilling and Beauchamp, which are not observed here.

The dominant reaction of Mo^+ with ethane at low energies is dehydrogenation, reaction 11. The cross-section for this process increases with increasing energy, consistent with an endothermic reaction or a reaction with a barrier. Above 1.5 eV, the $MoC_2H_4^+$ cross-section begins to decline, which can be attributed to depletion of the $MoC_2H_4^+$ product as the $MoC_2H_2^+$ product is formed in the endothermic double dehydrogenation, reaction 9. Above about 2.5 eV, the sum of the $MoC_2H_4^+$ and $MoC_2H_2^+$ product cross-sections begins to decline much more rapidly. This is apparently caused by competition with the formation of MoH^+ in reaction 2, suggesting that these reactions share a common intermediate.

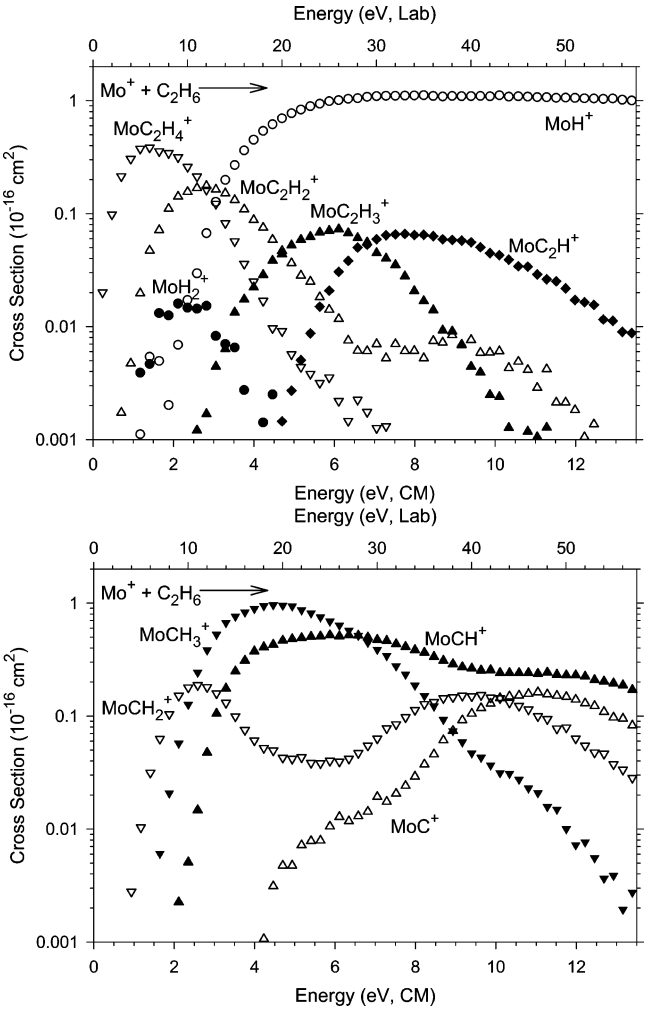

Figure 1. Cross-sections for reactions of Mo^+ with C_2H_6 as a function of kinetic energy in the center-of-mass frame (lower axis) and laboratory frame (upper axis). Panel a shows results for C−H bond cleavage reactions, and panel b shows results for C−C bond cleavage reactions.

At higher energies, $MoC_2H_3^+$ is formed in reaction 10. This species must come either from H atom loss from the $MoC_2H_4^+$ product or could evolve from dehydrogenation of $MoC_2H_5^+$. Although this latter product was looked for and not observed, it is possible that the $MoC_2H_5^+$ species loses H_2 readily such that its cross-section never reaches an appreciable magnitude. (Indeed, the thermochemistry measured indicates that dehydrogenation of $MoC_2H_5^+$ requires only 0.92 ± 0.21 eV, as confirmed by observations in the propane system; see next section.) The cross-section for $MoC_2H_3^+$ rises from an apparent threshold near 2.5 eV until near 6 eV where it begins to fall off. This decline is largely attributable to further dehydrogenation to form MoC_2H^+ in reaction 8. A competing dissociation

(65) Ervin, K. M.; Gronert, S.; Barlow, S. E.; Gilles, M. K.; Harrison, A. G.; Bierbaum, V. M.; DePuy, C. H.; Lineberger, W. C.; Ellison, G. B. *J. Am. Chem. Soc.* **1990**, *112*, 5750.

(66) Robinson, M. S.; Polak, M. L.; Bierbaum, V. M.; DePuy, C. H.; Lineberger, W. C. *J. Am. Chem. Soc.* **1995**, *117*, 6766.

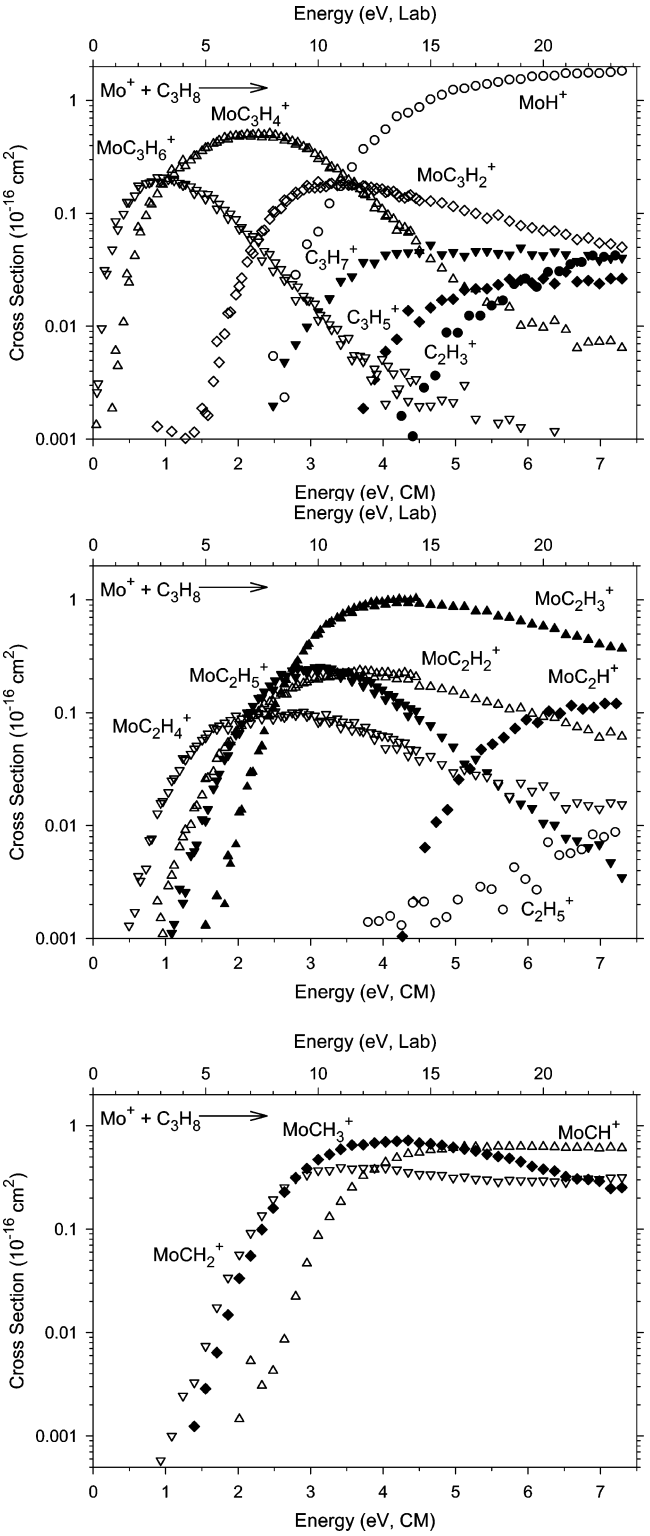

Figure 2. Cross-sections for reactions of Mo^+ with C_3H_8 as a function of kinetic energy in the center-of-mass frame (lower axis) and laboratory frame (upper axis). Panel a shows results for C−H bond cleavage reactions leading to $MoC_3H_x^+$, MoH^+, and hydrocarbon cation products; panel b shows results for C−C bond cleavage reactions leading to $MoC_2H_x^+$ and $C_2H_5^+$ products; and panel c shows results for C−C bond cleavage reactions leading to $MoCH_x^+$ products.

pathway is H atom loss to form $MoC_2H_2^+$, which can be seen as the shoulder in this cross-section starting near 6.5 eV.

One interesting minor product observed is MoH_2^+, formed in reaction 3. This process competes directly with dehydrogenation to form $MoC_2H_4^+$ in reaction 11. Clearly endothermic, this reaction reaches a maximum cross-section very close to the threshold observed for MoH^+ formation. The MoH_2^+ cross-section does not reach a maximum at this energy because this species decomposes to MoH^+, as this process corresponds to the overall formation of $MoH^+ + H + C_2H_4$, which cannot occur until 4.10 ± 0.06 eV. Therefore, the MoH_2^+ cross-section must decline at this energy because the MoH^+ channel depletes a common intermediate.

Figure 1b shows the products formed by cleavage of the C−C bond in ethane. The lowest energy product is the formation of $MoCH_2^+$, indicating the neutral product must be methane, reaction 6. This product cross-section rises sharply from an apparent threshold near 1 eV. The cross-section rises until near 2.5 eV and then declines before rising again near 6 eV. This latter feature must correspond to $CH_3 + H$ products, which can begin at $D_0(CH_3-H) = 4.55$ eV above the threshold for reaction 6. The $MoCH_3^+$ cross-section rises from an apparent threshold near 1.5 eV, continues rising to near 4.5 eV, and then falls off. The shape of the cross-section indicates that $MoCH_3^+$ decomposes by losing CH_3, a process that can begin at $D_0(CH_3-CH_3) = 3.90$ eV, and also by elimination of H_2 to form $MoCH^+$. A minor decomposition channel is also H atom loss to form $MoCH_2^+$, accounting for the high energy feature in the $MoCH_2^+$ cross-section. The $MoCH^+$ cross-section rises from an apparent threshold near 2.5 eV and reaches a plateau between 4 and 7 eV. It is likely that this cross-section is affected by decomposition of the $MoCH_3^+$ precursor to $Mo^+ + CH_3$. At very high energies, MoC^+ is also observed and is attributable to reaction 4. This can occur by H_2 loss from $MoCH_2^+$, explaining why two features are observed in this cross-section (i.e., with $CH_4 + H_2$ neutral products below about 8 eV and with $CH_2 + 2\ H_2$ neutral products at higher energies). It should be pointed out that the small magnitude of this product cross-section creates mass overlap problems with the much more intense $MoCH^+$ product channel. As a consequence, the detailed shape of the MoC^+ cross-section is unreliable, especially in the threshold region.

$Mo^+ + C_3H_8$. The reaction of the molybdenum cation with propane yields many products, as shown in Figure 2, which are accounted for by reactions 12−27.

$$Mo^+ + C_3H_8 \rightarrow MoH^+ + C_3H_7 \quad (12)$$

$$\rightarrow MoCH^+ + C_2H_5 + H_2 \quad (13)$$

$$\rightarrow MoCH_2^+ + (C_2H_4 + H_2) \quad (14)$$

$$\rightarrow MoCH_3^+ + C_2H_5 \quad (15)$$

$$\rightarrow MoC_2H^+ + CH_3 + 2H_2 \quad (16)$$

$$\rightarrow MoC_2H_2^+ + CH_4 + H_2 \quad (17)$$

$$\rightarrow MoC_2H_3^+ + CH_3 + H_2 \quad (18)$$

$$\rightarrow MoC_2H_4^+ + CH_4 \quad (19)$$

$$\rightarrow MoC_2H_5^+ + CH_3 \quad (20)$$

$$\rightarrow MoC_3H_2^+ + 3H_2 \quad (21)$$

$$\rightarrow MoC_3H_4^+ + 2H_2 \quad (22)$$

$$\rightarrow MoC_3H_6^+ + H_2 \quad (23)$$

$$\rightarrow C_2H_3^+ + MoH + CH_4 \quad (24)$$

$$\rightarrow C_2H_5^+ + MoCH_3 \quad (25)$$

$$\rightarrow C_3H_5^+ + MoH + H_2 \quad (26)$$

$$\rightarrow C_3H_7^+ + MoH \quad (27)$$

At the lowest energies in our study (~0.05 eV), we find essentially no reaction with a cross-section of $4.0 \pm 3.4 \times 10^{-19}$ cm^2, corresponding to a rate constant of $2.5 \pm 2.0 \times 10^{-14}$ cm^3/s. This result is consistent with the observations of Cassady and McElvany, who placed an upper limit for thermal reactions of 10^{-13} cm^3/s.[2] In contrast, Schilling and Beauchamp[1] report both reactions 22 and 23 with a branching ratio of 54:46 and a cross-section of 0.7×10^{-16} cm^2 at a center-of-mass energy of approximately 0.25 eV. At this energy, we find a cross-section of only $0.06 \pm 0.01 \times 10^{-16}$ cm^2 and a branching ratio of 4:96. We do not find nearly equal amounts of the $MoC_3H_4^+$ and $MoC_3H_6^+$ product ions until a kinetic energy of about 1.1 eV, where the total cross-section is 0.4×10^{-16} cm^2. These comparisons again indicate that the prior ion beam results correspond to higher kinetic energies than believed in the original study or that stabilizing secondary collisions drastically alter the products observed. The latter possibility is consistent with Schilling and Beauchamp reporting the observation of an $MoC_3H_8^+$ adduct (cross-section $= 0.8 \times 10^{-16}$ cm^2) at their energy of 0.25 eV, which we do not observe under our conditions. Presumably, the higher pressure conditions (5−10 times higher than used here) lead to collisional stabilization of these adducts in secondary collisions.

At low energies, the dominant products observed involve the loss of dihydrogen from the transient $MoC_3H_8^+$ intermediate to form $MoC_3H_x^+$ products as shown in Figure 2a. The primary product in this sequence is $MoC_3H_6^+$ formed by the dehydrogenation of propane in reaction 23. This species exhibits a small threshold for reaction, which could indicate an endothermic process or more likely a small barrier. The $MoC_3H_6^+$ cross-section reaches a maximum near 1 eV as the double dehydrogenation reaction 22 to form $MoC_3H_4^+$ becomes comparable in magnitude. As the energy is increased above about 2 eV, the $MoC_3H_4^+$ cross-section begins to decline as the endothermic triple dehydrogenation leading to the $MoC_3H_2^+$ product, reaction 21, begins. Above about 3 eV, the sum of the $MoC_3H_6^+$, $MoC_3H_4^+$, and $MoC_3H_2^+$ product cross-sections begins to decline, which we attribute to competition with the formation of MoH^+ in reaction 12.

C−H bond cleavage can also form the neutral MoH molecule accompanied by the $C_3H_7^+$ product, reaction 27. The alkyl fragment $C_3H_7^+$ rises from an apparent threshold near 2.5 eV. This product then dissociates by H_2 and CH_4 loss to form $C_3H_5^+$ and $C_2H_3^+$, respectively, in reactions 26 and 24.

The products formed by the cleavage of the C−C bond in the reaction of Mo^+ with propane are shown in Figure 2b,c. Reaction 19, loss of CH_4, has the lowest threshold of the various $MoC_2H_x^+$ products, followed shortly by an additional loss of H_2 in reaction 17. This species could be formed either by dehydrogenation of $MoC_2H_4^+$ or by demethanation of $MoC_3H_6^+$. The former appears to be the dominant pathway as the $MoC_2H_4^+$ cross-section declines as the $MoC_2H_2^+$ cross-section rises, but contributions from the latter pathway cannot be excluded.

The cross-section for $MoC_2H_5^+$ begins to rise near 1 eV and reaches a maximum at about 3 eV. The decline appears to be a result of dehydrogenation of this product ion to form $MoC_2H_3^+$, which starts near 1.7 eV. The $MoC_2H_3^+$ cross-section rises until near 4 eV and then declines. This is partly because of dehydrogenation to MoC_2H^+, reaction 16. The MoC_2H^+ cross-section rises from an apparent threshold near 4.2 eV and continues rising throughout the energy range examined. The sum of the $MoC_2H_x^+$ ($x = 5, 3, 1$) products begins to decline near 4 eV, corresponding to the energy required for the $MoC_2H_5^+$ species to decompose to $Mo^+ + C_2H_5$, 3.77 eV $= D_0(CH_3-C_2H_5)$. There is also a very small amount of $C_2H_5^+$ formed with an apparent threshold near 3 eV (not visible in Figure 2b). As $C_2H_5^+$ is not a viable dissociation product of $C_3H_7^+$, this product is attributed to reaction 25, in which the neutral $MoCH_3$ molecule is formed. Because of the small size of this cross-section, quantitative analysis of this product ion is not possible.

Figure 2c shows ionic products containing Mo and a single carbon atom. Of these, $MoCH_2^+$ is formed at the lowest energies. The $MoCH_2^+$ cross-section exhibits an apparent threshold near 1 eV with a small shoulder below 0.003 Å^2 and reaches a maximum near 3.5 eV. As observed in the reactions with methane and ethane, the $MoCH_2^+$ product probably decomposes by dehydrogenation to form MoC^+, but this product was sufficiently small that it was not monitored. $MoCH_3^+$ rises from an apparent threshold near 1.5 eV and falls off near 4 eV, largely because of dehydrogenation to form $MoCH^+$. This secondary product rises from an apparent threshold near 2.5 eV and plateaus at higher energies. These species are attributed to reactions 15 and 13, respectively.

Thermochemistry

The energy dependences of the various cross-sections are interpreted using eq 1. The optimum values of the parameters of eq 1 are listed for the ethane and propane systems in Tables 2 and 3, respectively. Each threshold can then be related to thermodynamic information assuming that this represents the energy of the product asymptote, an assumption that is usually correct for ion−molecule reactions because of the long-range attractive forces.[50] Thus, eq 28, where R−L is the reactant hydrocarbon, is used to derive the BDEs provided next.

$$D_0(Mo^+-L) = D_0(R-L) - E_0 \quad (28)$$

Because our bond energy determinations carefully include all sources of reactant energy, the thermochemistry obtained is for 0 K. As noted previously, the thermochemistry for $D_0(R-L)$ can be determined from information compiled elsewhere.[34,65,66]

In the following sections, our experimental BDEs and theoretical results for each of the product ions observed are compared with experimental and theoretical results from the literature. This thermodynamic information is summarized in Table 1. Relevant theoretical structures calculated here are provided in Figure 3. Detailed discussions of the theoretical

Table 2. Optimized Parameters of Eq 1 for $Mo^+ + C_2H_6$ System

reactants	products	σ_0	n	E_0 (eV)	$D_0(Mo^+-L)$ (eV)
$Mo^+ + C_2H_6$	$MoH^+ + C_2H_5$	1.85 (0.56)	1.4 (0.1)	2.81 (0.08)	1.50 (0.08)
	$MoH_2^+ + C_2H_4$	0.04 (0.01)	1.0 fixed	1.20 (0.15)	0.14 (0.15)
	$MoC^+ + CH_4 + H_2$	0.04 (0.01)	1.0 fixed	4.2 (0.2)	>3.2 (0.2)
	$MoC^+ + CH_3 + H + H_2$	0.91 (0.34)	1.0 fixed	8.22 (0.06)	>3.65 (0.06)
	$MoCH^+ + CH_3 + H_2$	2.51 (0.76)	0.8 (0.3)	3.12 (0.10)	5.29 (0.10)
	$MoCH_2^+ + CH_4$	0.47 (0.19)	2.3 (0.5)	1.14 (0.13)	>2.90 (0.13)
	$MoCH_3^+ + CH_3$	3.28 (0.91)	1.0 (0.1)	2.36 (0.04)	1.45 (0.04)
	$MoC_2H^+ + 2H_2 + H$	0.32 (0.10)	1.1 (0.2)	5.37 (0.16)	3.40 (0.16)
	$MoC_2H_2^+ + 2H_2$	0.53 (0.15)	1.2 (0.1)	1.21 (0.05)	1.87 (0.05)
	$MoC_2H_3^+ + H_2 + H$	0.13 (0.06)	1.6 (0.3)	2.96 (0.20)	3.14 (0.20)
	$MoC_2H_4^+ + H_2$	0.93 (0.27)	1.1 (0.1)	0.52 (0.03)	>0.82 (0.03)

Table 3. Optimized Parameters of Eq 1 for $Mo^+ + C_3H_8$ System

reactants	products	σ_0	n	E_0 (eV)	$D_0(Mo^+-L)$ (eV)
$Mo^+ + C_3H_8$	$MoH^+ + C_3H_7$	2.72 (0.56)	1.1 (0.1)	3.42 (0.05)	0.79 (0.05)
	$MoCH^+ + C_2H_5 + H_2$	1.30 (0.31)	1.4 (0.2)	2.99 (0.11)	5.38 (0.11)
	$MoCH_2^+ + C_2H_4 + H_2$	0.81 (0.10)	1.5 (0.2)	1.94 (0.12)	3.57 (0.12)
	$MoCH_2^+ + C_2H_6$	0.005 (0.002)	1.0 (0.2)	~1.0 (0.2)	>3.17 (0.2)
	$MoCH_3^+ + C_2H_5$	1.17 (0.15)	1.5 (0.1)	2.16 (0.06)	1.62 (0.06)
	$MoC_2H^+ + CH_3 + 2H_2$	0.50 (0.08)	0.8 (0.2)	5.12 (0.15)	3.11 (0.15)
	$MoC_2H_2^+ + CH_4 + H_2$	0.19 (0.07)	1.7 (0.2)	1.29 (0.10)	>1.25 (0.10)
	$MoC_2H_3^+ + CH_3 + H_2$	2.79 (0.28)	1.0 (0.1)	2.64 (0.08)	2.92 (0.09)
	$MoC_2H_4^+ + CH_4$	0.11 (0.02)	1.7 (0.4)	0.75 (0.12)	>0.05 (0.12)
	$MoC_2H_5^+ + CH_3$	0.74 (0.29)	2.0 (0.5)	1.69 (0.14)	2.09 (0.14)
	$MoC_3H_2^+ + 3H_2$	0.55 (0.04)	1.2 (0.4)	2.12 (0.13)	4.34 (0.21)
	$MoC_3H_4^+ + 2H_2$	0.60 (0.02)	1.4 (0.1)	0.64 (0.03)	2.22 (0.03)
	$MoC_3H_6^+ + H_2$	0.57 (0.13)	1.2 (0.1)	0.41 (0.05)	>0.81 (0.05)
	$C_2H_3^+ + MoH + CH_4$	0.12 (0.06)	1.2 (0.1)	4.66 (0.11)	2.05 (0.12)
	$C_3H_5^+ + MoH + H_2$	0.08 (0.01)	0.9 (0.2)	3.95 (0.13)	2.07 (0.16)
	1-$C_3H_7^+ + MoH$	0.12 (0.03)	1.3 (0.4)	2.77 (0.18)	2.49 (0.18)
	2-$C_3H_7^+ + MoH$	0.12 (0.03)	1.3 (0.4)	2.77 (0.18)	1.71 (0.18)

results for MoH^+ and $MoCH_x^+$ ($x = 0-3$) can be found elsewhere[36] and are briefly reviewed here. Additional theoretical results are found in the Supporting Information, which includes the energies and ZPE of all reactants and products calculated using several levels of theory (Table S1), as well as energies and ZPE (Table S2) and geometries (Table S3) of ground- and excited state species calculated at the B3LYP/HW level.

MoH^+. This product is formed in both systems. A reliable value for $D_0(Mo^+-H)$ (Table 1) has previously been determined from the reactions of Mo^+ with H_2 and D_2.[37] This value is in reasonable agreement with high level theoretical calculations,[43,68−70] including our own B3LYP and QCISD(T) calculations.[36] Using this BDE, the predicted thresholds for the formation of MoH^+ are 2.59 ± 0.06 and 2.49 ± 0.06 eV in the C_2H_6 and C_3H_8 systems, respectively. The threshold measured in the ethane system, Table 2, is higher by 0.22 ± 0.10 eV, just outside the combined uncertainties, whereas that for the propane system is well above the predicted value (Table 3). Such shifts can be attributed to competition with more favorable dehydrogenation processes for each reaction system.

All theoretical calculations[36,43,68−70] agree that the ground state for MoH^+ is $^5\Sigma^+$ with a valence electron configuration of $\sigma_b^2\pi^2\delta^2$, in which the bonding orbital is σ_b and the π and δ orbitals are molybdenum-based 4d orbitals. Excited states all lie over 1 eV higher in energy.[36]

MoC^+. The MoC^+ BDE has been measured previously as 4.31 ± 0.20 eV from the endothermicity of the $Mo^+ + CO \rightarrow MoC^+ + O$ reaction.[38] In our work on the CH_4 system, the threshold obtained from the MoC^+ cross-section results in $D_0(Mo^+-C)$ of 4.62 ± 0.11 eV. The weighted average of these two values is 4.55 ± 0.19 eV (where the uncertainty is twice the standard deviation from the mean) and is our best experimental value.

As noted previously, the detailed shape of the MoC^+ cross-section, especially in the critical threshold region, is unreliable in the ethane system because of mass overlap problems. Nevertheless, it is clear that two features are observed, corresponding to neutral products of $CH_4 + H_2$ and $CH_3 + H + H_2$, but the measured thresholds (Table 2) are somewhat higher than predicted from the thermochemistry ascertained previously, 2.84 ± 0.19 and 7.32 ± 0.19 eV, respectively. For the low energy component, this may be a result of the inaccurate cross-section in the threshold region, whereas the higher energy component may be shifted by competition with the much more favorable processes occurring at lower energies.

Calculations[36] indicate that the ground state of MoC^+ is $^2\Delta$, with a valence configuration (ignoring the C(2s) electrons) of $\sigma_b^2\pi_b^4\delta^1$, where the σ_b and π_b orbitals are Mo−C bonding and the δ orbital is a Mo-based 4d nonbonding orbital. A low lying excited state, $^4\Sigma^+$ ($\sigma_b^1\pi_b^4\delta^2$), lies 0.17−0.59 eV higher in energy depending on the level of theory used.

$MoCH^+$. As noted previously, the mechanism for formation of $MoCH^+$ is dehydrogenation of the primary $MoCH_3^+$ product. The thresholds obtained from the $MoCH^+$ cross-sections result in $D_0(Mo^+-CH)$ of 5.12 ± 0.30, 5.29 ± 0.10, and 5.38 ± 0.11 eV for the CH_4,[36] C_2H_6, and C_3H_8 systems, respectively. Our best value for $D_0(Mo^+-CH)$ is the weighted average of all three values yielding 5.32 ± 0.14 eV, where the uncertainty is two standard deviations of the mean. Theory[36] finds that $MoCH^+$ has a covalent triple bond with a linear geometry and a $^3\Sigma^+$ ($\sigma_b^2\pi_b^4\delta^2$) ground state, where the character of the orbitals is the same as MoC^+. Excited states are all calculated to lie >0.9 eV higher in energy.

(67) Ref deleted in proof.
(68) Schilling, J. B.; Goddard, W. A., III; Beauchamp, J. L. *J. Am. Chem. Soc.* **1987**, *109*, 5565.
(69) Pettersson, L. G. M.; Bauschlicher, C. W., Jr.; Langhoff, S. R.; Partridge, H. *J. Chem. Phys.* **1987**, *87*, 481.
(70) Siegbahn, P. E. M.; Blomberg, M. R. A.; Svensson, M. *Chem. Phys. Lett.* **1994**, *223*, 35.

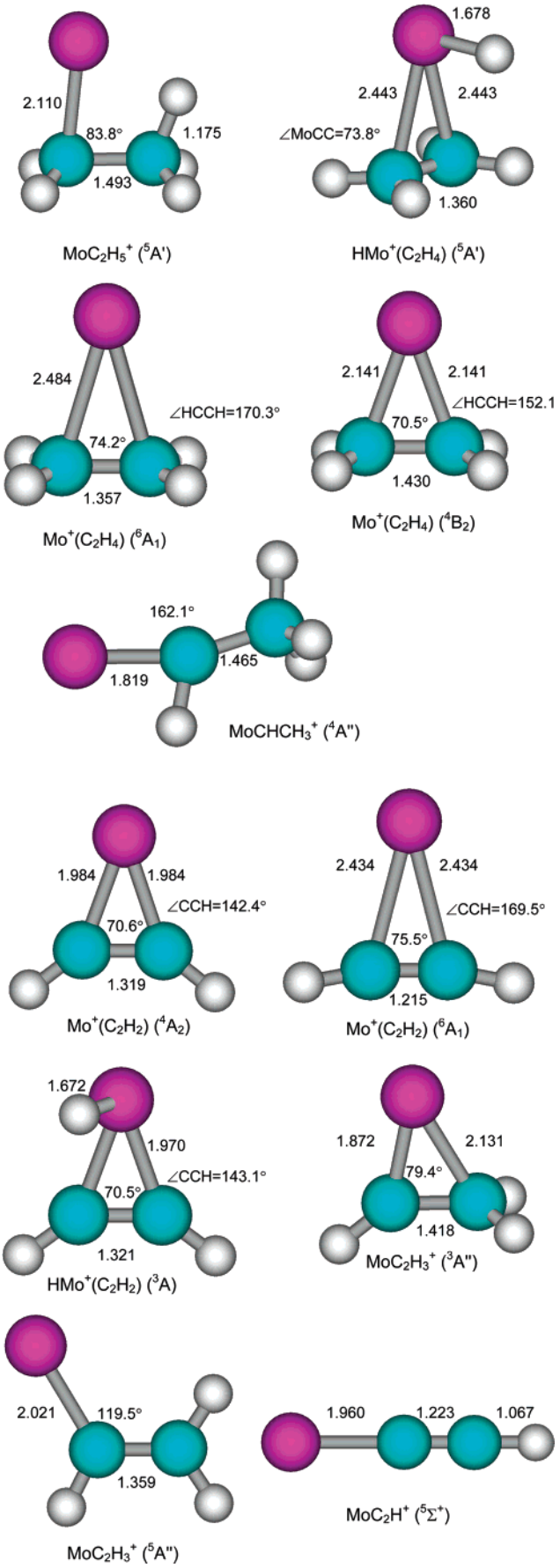

Figure 3. Theoretical structures of $MoC_2H_x^+$ species ($x = 1-5$) calculated at the B3LYP/HW/6-311++G(3df,3p) level of theory. Bond lengths are in angstroms.

$MoCH_2^+$. As previously reported,[36] generation of $MoCH_2^+$ by dehydrogenation of methane is the dominant process in this system; thus, the threshold for this reaction provides a reliable determination of the BDE, $D_0(Mo^+-CH_2) = 3.57 \pm 0.10$ eV. Given this bond energy, the formation of $MoCH_2^+ + CH_4$ in the ethane system should have a threshold of 0.47 ± 0.10 eV but is not observed until 0.67 ± 0.16 eV higher in energy (Table 2). Either this reaction has a barrier, as has been observed for the neighboring elements, Zr^+ and Nb^+,[29,30] or competition with the more favorable dehydrogenation reaction has suppressed this reaction at threshold. The theoretical potential energy surfaces detailed in the following paper on reaction mechanisms finds that a barrier is indeed present for this reaction.

At higher energies, another prominent feature in the $MoCH_2^+$ cross-section is observed. If this is identified as a decomposition product of the primary $MoCH_3^+$ product, then the overall reaction is $MoCH_2^+ + H + CH_3$, which should have a threshold of 4.95 ± 0.10 eV, consistent with the apparent onset for this cross-section feature. In the propane system, $MoCH_2^+$ could be formed with C_2H_6 or $C_2H_4 + H_2$ as neutral products. For the neighboring metal ion, Nb^+, both processes were observed with the latter being more efficient by a factor of about 2 orders of magnitude.[30] A similar result is obtained here. If the main part of the $MoCH_2^+$ cross-section is reproduced using eq 1, then a threshold of 1.94 ± 0.12 eV is obtained. If this threshold is identified with the $C_2H_4 + H_2$ products, the value for $D_0(Mo^+-CH_2)$ derived is 3.57 ± 0.12 eV, in good agreement with the value derived from the methane system. However, this model of the data fails to reproduce a small shoulder on the low energy side of the $MoCH_2^+$ cross-section (Figure 2c). Because of its small size, modeling this cross-section cannot be done unequivocally, but if the parameter n is fixed at unity, then a threshold of about 1.0 eV is obtained with a magnitude (σ_0) about 160 times smaller than the main cross-section feature, Table 1. This threshold does not correspond to the thermodynamic threshold for the production of $MoCH_2^+ + C_2H_6$, which can begin at 0.60 ± 0.10 eV, suggesting a barrier to the overall process. This conclusion is confirmed by the theoretical study in the following paper.[71]

Theory indicates that $MoCH_2^+$ has a covalent double bond leading to a $^4B_1$ ground state, with a valence electron configuration of $(1a_{1b})^2(1b_{1b})^2(2a_1)^1(1a_2)^1(1b_2)^1$, where the $1a_{1b}$ and $1b_{1b}$ orbitals are the Mo−C σ and π bonds, and the remaining orbitals are metal-based nonbonding 4d orbitals.[36,72] The theoretical results of Bauschlicher et al. provide a best estimate for $D_0(Mo^+-CH_2)$ of 3.08 ± 0.17 eV,[72] whereas our B3LYP/HW* and QCISD(T)/HW* calculations find values of 3.22 and 3.35 eV, respectively.[36] All excited states of the molybdenum carbene cation lie over 1.1 eV higher in energy, although a molecule having the alternate $HMoCH^+$ ($^2A''$) structure lies 0.72 eV higher.[36]

$MoCH_3^+$ and $MoC_2H_5^+$. The thresholds obtained for the $MoCH_3^+$ cross-sections in the CH_4,[36] C_2H_6, and C_3H_8 systems result in $D_0(Mo^+-CH_3)$ of 1.63 ± 0.12 (after correction for competitive shifts),[36] 1.45 ± 0.04, and 1.62 ± 0.06 eV, respectively. The weighted average of these three values is 1.57 ± 0.09 eV (two standard deviations of the mean). This value compares reasonably well with the theoretical value of 1.38 ± 0.13 eV given by Bauschlicher et al.,[41] 1.31 eV by Schilling et al.,[73] and our calculated values of 1.70 (QCISD(T)/HW) to 1.80

(71) Armentrout, P. B. *Organometallics* **2007**, *26*, 5486.
(72) Bauschlicher, C. W., Jr.; Partridge, H.; Sheehy, J. A.; Langhoff, S. R.; Rosi, M. *J. Phys. Chem.* **1992**, *96*, 6969.
(73) Schilling, J. B.; Goddard, W. A.; Beauchamp, J. L. *J. Am. Chem. Soc.* **1987**, *109*, 5573.

(B3LYP/HW*).[36] This identifies this species as the molybdenum methyl cation, which has a single covalent molybdenum carbon bond and a $^5A_1$ ground state having C_{3v} symmetry. We also found a $^3A'$ state lying 0.99 eV higher in energy, which has a weak agostic interaction distorting it from C_{3v} symmetry.[36] The alternate structures of $HMoCH_2^+$ ($^3A''$) and $(H)_2MoCH^+$ (^3A) lie fairly close in energy (0.07 and 0.13 eV above the $^3A'$ state).

In the propane system, cleavage of the C−C bond yields $MoC_2H_5^+$ in competition with $MoCH_3^+$. Inspection of the data indicates that the threshold for process 20 is below that for reaction 15 (Figure 2b,c). Analysis of the $MoC_2H_5^+$ cross-section is complicated because this product dehydrogenates at slightly higher energies to form $MoC_2H_3^+$. Nevertheless, similar thresholds are obtained whether we analyze the $MoC_2H_5^+$ cross-section independently or the sum of the $MoC_2H_5^+$ and $MoC_2H_3^+$ cross-sections. The results in Table 3 lead to $D_0(Mo^+-C_2H_5) = 2.09 \pm 0.14$ eV, 0.52 ± 0.17 eV greater than $D_0(Mo^+-CH_3)$. This is considerably higher than results for the first-row congener of molybdenum, where $D_0(Cr^+-C_2H_5) = D_0(Cr^+-CH_3) + 0.19$ eV.[11] Nevertheless, theory confirms such a large difference, giving BDE differences, $D_0(Mo^+-C_2H_5) - D_0(Mo^+-CH_3)$, of 0.33 eV at the B3LYP level and 0.62 eV at the QCISD(T) level for both the HW and the HW* basis sets. $Mo^+-C_2H_5$ BDEs are predicted to range from 2.09−2.37 eV (B3LYP/HW − QCISD(T)/HW*), in good agreement with the experimental value.

Although the structure of $CrC_2H_5^+$ has not been examined theoretically, the structure of the $^5A'$ ground state of $MoC_2H_5^+$ (Figure 3) suggests why the bond to Mo is relatively strong. Rather than finding a MoCC bond angle comparable to the MoCH bond angles ($\angle$Mo−C−H = 112.7° in $MoC_2H_5^+$ and 108.8° in $MoCH_3^+$), the molybdenum is bent over strongly giving $\angle$Mo−C−C = 83.8°. Further, Mo^+ is also interacting with a hydrogen atom on this methyl group such that r_{MoH} = 1.975 Å, thereby extending this C−H bond to 1.175 Å versus 1.087 Å for the other two Cβ−H bonds. Rotating this hydrogen away from the molybdenum (such that there is a MoCCH dihedral angle of 180° instead of 0°) costs 0.19 eV (B3LYP/HW) and forms a $^5A'$ state ($\angle$Mo−C−C = 84.7°). This state has an imaginary frequency of 296 cm^{-1} corresponding to a methyl torsion that collapses back to the $^5A'$ ground state. A geometry similar to the $^5A'$ ground state is also found for an excited ^3A state ($\angle$Mo−C−C = 83.5° and r_{MoH} = 1.948 Å), which lies 0.92 eV higher in energy, as might be expected according to Hund's rules for a species having four nonbonding electrons. A singlet excited state lying 1.15 eV higher than the ground state was also found, but this has a hydrido ethylidene structure ($H-Mo^+=CHCH_3$).

We also considered whether the ground state geometry of $MoC_2H_5^+$ is not the molybdenum ethyl cation but rather $HMo^+(C_2H_4)$, a hydrido−ethene complex (Figure 3). The lowest energy species of this isomer is a $^5A'$ state lying 0.28 eV above $MoC_2H_5^+$ ($^5A'$). The geometry in this species exhibits a Mo−H bond distance of 1.678 Å, comparable to that found for MoH^+ ($^5\Sigma^+$), 1.673 Å, and a C−C bond distance, 1.360 Å, only slightly extended from the 1.325 Å calculated for free ethene. The carbon atoms of the ethene ligand lie in a plane perpendicular to the MoH bond axis, presumably to avoid the sd hybrid orbital on Mo used to form the MoH covalent bond. Alternate spin states, $^3A''$, $^1A''$, $^3A'$, and $^1A'$, were also found for $HMo^+(C_2H_4)$ and lie 0.69, 1.05, 1.10, and 1.74 eV, respectively, above $MoC_2H_5^+$ ($^5A'$). These states have more extended C−C bonds, 1.433, 1.431, 1.396, and 1.415 Å, respectively, consistent with more covalent metal−ethene binding interactions expected for the lower spin states.

Products of Dehydrogenation: Molybdenum Alkene Cations. Dehydrogenation of ethane and propane by Mo^+ exhibit thresholds that suggest that $D_0(Mo^+-C_2H_4) = 0.82 \pm 0.03$ eV and $D_0(Mo^+-C_3H_6) = 0.81 \pm 0.05$ eV. These alkene BDEs are very similar to one another, as also observed for other transition-metal ions,[11] but are considerably lower than those for the adjoining early second-row transition-metal ions, $D_0(Zr^+-C_2H_4) = 2.84 \pm 0.18$ eV[29] and $D_0(Nb^+-C_2H_4) = 2.8 \pm 0.3$ eV.[30] Because both ground state Zr^+ (^4F, $5s^14d^2$) and Nb^+ (^5D, $4d^4$) have an empty d orbital that can be used to accept electron density from the alkene, whereas Mo^+ (^6S, $4d^5$) does not, it is reasonable that the metal ion alkene BDEs for molybdenum would be less than those of zirconium and niobium. For instance, for the first-row congeners, the metal ion−ethene BDEs for titanium, vanadium, and chromium, have been measured as 1.51 ± 0.11, 1.29 ± 0.08, and 0.99 ± 0.11 eV, respectively.[74] Even so, the Mo^+−alkene BDEs seem very weak, even smaller than those for Cr^+. It is possible that the large BDEs for Zr^+ and Nb^+ are a result of a low spin metallacycle species, as compared to an electrostatically bound high spin state for Mo^+. Overall, we conclude that the BDEs determined here for ethene and propene are likely to be lower limits, a conclusion supported by the potential energy surface for these reactions discussed in the following paper.[71] Given a bond energy near 0.8 eV, loss of methane in the reaction with propane to form $MoC_2H_4^+$ should be thermoneutral or slightly exothermic but instead exhibits an appreciable barrier of 0.75 ± 0.12 eV (Table 3). This is comparable to the observation that the loss of methane from ethane also exhibits a barrier of 0.67 ± 0.16 eV.

A further indication that the Mo^+−alkene BDEs are lower limits comes from our calculations. Here, the ground state for $Mo^+(C_2H_4)$ is found to be $^6A_1$ with a BDE of 1.26−1.39 eV, considerably stronger than measured here. The first excited state is $^4B_2$, lying only 0.51 eV higher in energy, with the $^4A_2$, $^4B_1$, $^4A_1$, and $^2B_2$ excited states at 1.12, 1.13, 1.18, and 1.18 eV, respectively (Table S2). Note that because the Mo^+ (^4G) asymptote is calculated to lie 1.92 eV higher than Mo^+ (^6S), this indicates that the $Mo^+-C_2H_4$ bond along the quartet surface is stronger than along the sextet surface by 1.41 eV (bond energies of 2.67 eV vs 1.26 eV), consistent with the more covalent bonding character allowed by the low spin on the metal ion. This is also indicated by the C−C bond distances of 1.357 Å for $^6A_1$, only slightly extended from that for free ethene, 1.325 Å, versus those for the low spin states of 1.42−1.43 Å [Figure 3 (except the $^4A_1$ state also has a short bond length of 1.358 Å) and Table S3].

Two alternate structures for $[Mo,2C,4H]^+$ were also explored. The molybdenum ethylidene cation, $Mo^+=CHCH_3$, was found to have a $^4A''$ ground state and lies 0.76 eV above the $^6A_1$ state of $Mo^+(C_2H_4)$ (Table S2). A $^4A'$ state lies another 1.14 eV higher in energy. The hydrido vinyl structure, $HMoC_2H_3^+$, was also located. Both ^4A and ^2A states were found and lie 1.24 and 1.84 eV, respectively, higher in energy than $Mo^+(C_2H_4)$ ($^6A_1$) (Table S2).

Products of Dehydrogenation: Molybdenum Alkyne Cations. Subsequent dehydrogenation of the $MoC_2H_4^+$ product formed in the ethane and propane systems is also observed, with thresholds that convert to $D_0(Mo^+-C_2H_2) = 1.87 \pm 0.05$ and 1.25 ± 0.10 eV, respectively. The lower value in the latter

(74) Sievers, M. R.; Jarvis, L. M.; Armentrout, P. B. *J. Am. Chem. Soc.* **1998**, *120*, 1891.

system may be an additional consequence of the barrier observed for the formation of the $MoC_2H_4^+$ product in the propane system. Sodupe and Bauschlicher have calculated a BDE of 0.85 eV for the $^6A_1$ state of $MoC_2H_2^+$ and 0.68 eV for the $^4A_2$ state but suggest that the latter state is actually the true ground state.[44] (It can be noted that the BDEs calculated in this work are typically low, by factors of 1.3−2.1 for first-row transition-metal ions because the geometry was calculated at too low a level.) This prediction is borne out by the more advanced calculations performed here, which obtain a $^4A_2$ ground state with a BDE of 1.47−1.59 eV, only slightly below the value measured here, and a $^6A_1$ state lying 0.28−0.37 eV higher in energy. These species have C−C bond distances of 1.319 and 1.215 Å and C−C−H bond angles of 142.4 and 169.5° (Figure 3) as compared to free ethyne, 1.196 Å and 180.0°. Both geometric quantities indicate more covalent metal−ligand interactions in the lower spin state, making it more like a metallacycle. Additional excited states, $^4B_2$, $^2A_1$, $^4B_1$, and $^6A_2$, having excitation energies of 0.53, 0.85, 1.22, and 2.90 eV, respectively, were also located (Table S2). We also considered whether these ions could possibly have a $Mo^+{=}C{=}CH_2$ connectivity. These structures are stable minima, but the lowest energy state, $^4B_2$, lies 0.51 eV above the $^4A_2$ state of the metal alkyne geometry. Excited states of $MoCCH_2^+$, $^4B_1$, $^4A_1$, and $^4A_2$ lie 0.83, 1.32, and 2.15 eV above the $^4B_2$ state.

Double dehydrogenation of propane is also endothermic and yields a threshold indicating that $D_0(Mo^+{-}C_3H_4) = 2.22 \pm 0.03$ eV, presuming that C_3H_4 has a propyne structure (2.28 ± 0.03 eV for allene). The propyne structure seems likely given that double dehydrogenation of ethane (also a relatively efficient process) occurs, and theory suggests that this corresponds to the ethyne ligand. This high bond energy further substantiates the larger BDE for $Mo^+{-}(C_2H_2)$, although the difference of 0.35 ± 0.06 eV between the 2.22 ± 0.03 eV BDE for propyne and 1.87 ± 0.05 eV for ethyne seems a bit high. This suggests that the latter value may be a lower limit, which agrees with the theoretical potential energy surface obtained in the following paper.[71] As discussed there, the enhanced stability of intermediates and transition states for the longer hydrocarbon suggest that the value for propyne probably corresponds to the thermodynamic limit.

Triple dehydrogenation to form $MoC_3H_2^+$ is also observed as an endothermic process. Here, the difficulty is assigning a likely structure to this species, although a reasonable possibility is the $C{=}C{=}CH_2$ biradical. Assuming this dissociation asymptote, the thermochemistry measured here provides a $Mo^+{=}C_3H_2$ BDE of 4.34 ± 0.21 eV, somewhat stronger than $D_0(Mo^+{-}CH_2) = 3.57 \pm 0.10$ eV. This is plausible as the Mo−C double bond can be augmented by delocalization of the C−C π electrons into a half-filled dπ nonbonding orbital on molybdenum.

MoH_2^+. One of the more interesting minor products observed in these systems is MoH_2^+. A comparable product is not observed in the reactions of first-row transition-metal cations with alkanes but has been observed for reactions of third-row metal cations.[75,76] The MoH_2^+ product is observed in only the C_2H_6 system (Figure 1a) and must be accompanied by ethene as the neutral product, reaction 3. The threshold obtained from the MoH_2^+ cross-section yields $D_0(Mo^+{-}H_2) = 0.14 \pm 0.15$ eV. If the MoH_2^+ species is a dihydride with two covalent MoH bonds, then this BDE can be converted to $D_0(Mo^+{-}2H) = 4.62 \pm 0.15$ eV. When this bond energy sum is combined with $D_0(Mo^+{-}H) = 1.72 \pm 0.06$ eV[37] (Table 1), the second covalent BDE can be determined as $D_0(HMo^+{-}H) = 2.90 \pm 0.16$ eV. This striking difference in the first and second covalent bonds is unreasonable and suggests that MoH_2^+ is the electrostatically bound dihydrogen complex, $Mo^+(H_2)$. For comparison, Bowers and co-workers have measured the binding of H_2 to Nb^+ and determined a BDE of 0.64 eV.[77] One expects that the $Mo^+{-}H_2$ BDE should be weaker because the $4d^5$ electronic configuration of $Mo^+(^6S)$ necessarily occupies the 4dσ orbital pointed at the dihydrogen molecule, whereas $Nb^+(^5D, 4d^4)$ can leave this orbital unoccupied.

The conclusion that the MoH_2^+ species observed here is the electrostatically bound $Mo^+(H_2)$ complex is verified by theory. Schilling et al. first characterized MoH_2^+ and found a $^4B_2$ state having two minima, one at a H−Mo−H bond angle of 65° and a second at 112°.[78] This species was found to lie about 1.5 eV above the $Mo^+ + H_2$ asymptotic energy. Das and Balasubramanian (DB)[43] explored the various states of MoH_2^+ more thoroughly and found only one species below the Mo^+ (^6S) + H_2 asymptote, the electrostatically bound $Mo^+(H_2)$ ($^6A_1$) species having a H−Mo−H bond angle near 20° and a well-depth of about 0.2 eV (details of this state are not provided, see Figure 2 of ref 43). The $^4B_2$ state characterized by Schilling et al. is the lowest inserted dihydride state, which DB calculate lies 0.87 eV below the Mo^+ (^4G) + H_2 excited state asymptote, which places it approximately 1.0 eV above the Mo^+ (^6S) + H_2 ground state asymptote. Our own calculations come to a similar conclusion. The lowest energy state of MoH_2^+ is the $^6A_1$ state having an intact H_2 bond and a well-depth of 0.25−0.31 eV, in good agreement with the experimental energy of 0.14 ± 0.15 eV. The first dihydride state is again the $^4B_2$ state, which lies 0.74−1.10 eV above the Mo^+ (^6S) + H_2 asymptote.

$MoC_2H_x^+$ (x = 1 and 3). The thresholds obtained for $MoC_2H_3^+$ in the reactions with C_2H_6 and C_3H_8 give $D_0(Mo^+{-}C_2H_3)$ of 3.14 ± 0.20 and 2.92 ± 0.09 eV, respectively. We adopt the weighted average, 2.95 ± 0.15 eV, as our best value (with an uncertainty of two standard deviations of the mean). Note that this BDE is greater than that for the single bond in $Mo^+{-}CH_3$, 1.57 ± 0.09 eV, but less than the double bond of $Mo^+{-}CH_2$, 3.57 ± 0.10 eV. As discussed elsewhere,[11] the transition-metal ion bonds to vinyl can be strengthened by delocalization of the C−C π electrons to the metal center (i.e., a dative bond in addition to the covalent bond). For the early first-row transition-metal cations (Ti^+, V^+, and Cr^+) where there is an empty orbital to accept these electrons, this bond to vinyl is 1.42 ± 0.35 eV stronger than the bond to methyl, very similar to the enhancement here of 1.38 ± 0.18 eV. Alternatively, this species could correspond to the $HMo^+(C_2H_2)$ isomer. The thermochemistry measured here indicates that $D_0(HMo^+{-}C_2H_2) = 2.69 \pm 0.17$ eV and $D_0[HMo^+(C_2H_2)] = 2.54 \pm 0.16$ eV. Both of these BDEs are 0.8 eV above the isolated $Mo^+{-}C_2H_2$ and $Mo^+{-}H$ bond energies. If correct, then this enhancement must occur as a consequence of the sd hybridization involved in both individual bonds. Namely, formation of the 5s−4d hybrid orbital that binds to the H atom also forms a second 5s−4d orbital perpendicular to the first one but empty. This empty sd hybrid is apparently a better acceptor orbital than the

(75) Zhang, X.-G.; Liyanage, R.; Armentrout, P. B. *J. Am. Chem. Soc.* **2001**, *123*, 5563.

(76) Li, F.-X.; Zhang, X.-G.; Armentrout, P. B. *Int. J. Mass Spectrom.* **2006**, *255−256*, 279.

(77) Bowers, M. T.; Kemper, P. R.; van Koppen, P.; Wyttenbach, T.; Carpenter, C. J.; Weis, P.; Gidden, J. In *Energetics and Structures of Gas Phase Ions: Macromolecules, Clusters and Ligated Transition Metals*; Minas de Piedade, M. E., Ed.; Kluwer: Dordrecht, The Netherlands, 1999; p 235.

(78) Schilling, J. B.; Goddard, W. A.; Beauchamp, J. L. *J. Phys. Chem.* **1987**, *91*, 4470.

empty 5s orbital of Mo^+ (^6S). Thus, the hybridization is made more efficient and effective because both ligands are present.

According to our theoretical calculations, the lowest energy $MoC_2H_3^+$ species has the $HMo^+(C_2H_2)$ geometry (Figure 3), with a triplet spin state and a $Mo^+-C_2H_3$ BDE of 2.16 eV (B3LYP/HW) to 2.50 (QCISD(T)/HW*) eV, somewhat below the experimental value. The $HMo^+-C_2H_2$ and $H-Mo^+(C_2H_2)$ bond energies range from 1.92 to 2.36 and 2.34 to 2.38 eV, respectively, and are 0.45−0.76 eV stronger than the calculated BDEs for $Mo^+-C_2H_2$ and Mo^+-H. A ^1A state having the $HMo^+(C_2H_2)$ geometry was also located only 0.45 eV higher in energy, whereas the analogous $^5A'$ state lies 0.46 eV above the ground state (Table S2). In all three spin states, the MoH bond length is essentially unchanged from that for MoH^+ ($^5\Sigma^+$), 1.67 Å (Figure 3 and Table S3). In the quintet and singlet states, the MoH bond lies nearly perpendicular to the plane established by the Mo−ethyne complex, whereas in the triplet state, this angle is about 65°. This geometry is consistent with the utilization of the two 5s−4d hybrids as the bonding orbitals as suggested previously. As might be expected, the distortion of the ethyne molecule is substantial for the lower spin states (∠C−C−H = 169° for $^5A'$, 143° for ^3A, and 144° for $^1A'$), indicative of more covalent interactions.

In contrast, the lowest energy molybdenum vinyl species was a $^5A''$ state lying 0.32 (B3LYP/HW) to 0.64 (QCISD(T)/HW*) higher in energy. BDEs for this species ranged from 1.83 eV (B3LYP/HW) to 1.91 (QCISD(T)/HW) eV, well below the experimental value. This species has a planar geometry in which Mo^+ essentially replaces a hydrogen atom of ethene, ∠Mo−C−C = 119.5° (Figure 3). Excited states for this species lying 0.30 ($^3A''$), 0.82 ($^3A'$), 1.01 ($^3A''$), and 1.43 (^1A) eV above the $MoC_2H_3^+$ ($^5A''$) state were also located (Table S2). The higher lying $^3A''$ and ^1A states are the lower spin analogues of the quintet state, having geometries in which Mo^+ bends over to interact with the unsaturated C−C bond while maintaining nearly planar geometries, ∠Mo−C−C = 94° for $^3A''$ and ∠Mo−C−C = 77° for ^1A (Table S3). The two low lying triplet states have very different geometries (no longer planar) in which Mo^+ interacts with the C−C π cloud of vinyl, ∠Mo−C−C = 79° for both $^3A''$ and $^3A'$ (Figure 3).

MoC_2H^+ is measured to have thresholds that yield $D_0(Mo^+-C_2H) = 3.40 \pm 0.16$ and 3.11 ± 0.15 eV in the ethane and propane systems, respectively. The reasonable agreement between these two values leads us to assign the average of 3.25 ± 0.22 eV as our best value for $D_0(Mo^+-C_2H)$. This BDE is much stronger than $D_0(Mo^+-CH_3)$ and comparable to $D_0(Mo^+-CH_2)$, suggesting it has double bond character. Presuming that this species has a $Mo^+-C\equiv CH$ structure, this can occur by delocalization of both pairs of C−C π electrons into the dπ orbitals on Mo^+, in essence forming two dative bonds in addition to the covalent Mo−C single bond. The theoretical calculations confirm this, finding a linear $^5\Sigma^+$ ground state and a BDE of 3.57 eV (QCISD(T)/HW) to 3.64 (B3LYP/HW*) eV, in reasonable agreement with experiment. The Mo−C bond length of 1.960 Å (Figure 3) lies between those for $MoCH_2^+$ ($^4B_1$) and $MoCH_3^+$ ($^5A_1$), 1.880 and 2.104 Å, respectively. Excited states of this molecule were also identified: $^5\Pi$ (0.42 eV), $^3\Sigma$ (0.89 eV), $^5\Delta$ (1.03 eV), and $^3\Delta$ (2.16 eV) (Table S2).

MoH. In the propane system, the $C_2H_3^+$, $C_3H_5^+$, and $C_3H_7^+$ species are formed in reactions 24, 26, and 27 along with MoH. When combined with literature thermochemistry for the hydrocarbon ions[34] and the ionization energy of molybdenum, IE(Mo) = 7.092 eV,[79] the measured thresholds for these reactions result in $D_0(Mo-H) = 2.05 \pm 0.12$, 2.07 ± 0.16, and 1.71 ± 0.18 eV, respectively. Apparently, the threshold for the latter process (assigned to formation of 2-$C_3H_7^+$) is elevated because of competition with dehydrogenation and $MoH^+ + C_3H_7$, making it a lower limit. The agreement between the other two values, which have a weighted average of $D_0(Mo-H) = 2.06 \pm 0.19$ eV, suggests that this may correspond to the thermodynamic value. Indeed, this value agrees well with the brackets of 1.94 ± 0.09 eV ≤ $D_0(Mo-H)$ ≤ 2.06 ± 0.09 eV, as determined previously by Sallans et al. using proton-transfer reactions with Mo^-.[39] An alternate experimental value of 2.08 eV ≤ $D_0(Mo-H)$ ≤ 2.52 eV was reported on the basis of hydride transfer reactions with Mo^+ from the preliminary work of Schilling and Beauchamp but was never published independently with experimental details provided.[22] Note that the two bracketing experiments do overlap in the vicinity of a BDE of 2.1 eV, in agreement with the value measured here. Given that $D_0(Mo-H) = 2.06 \pm 0.19$ eV and $D_0(Mo^+-H) = 1.72 \pm 0.06$ eV, we can also derive the ionization energy of MoH as 7.43 ± 0.20 eV.

Langhoff et al. calculated a $^6\Sigma^+$ ground state for MoH with a valence molecular orbital configuration of $\sigma_b^2\pi^2\delta^2\sigma^1$, where the bonding orbital is largely Mo(5s)−H(1s) and the other orbitals are all 4d orbitals on Mo.[40] They find 0 K BDEs of 1.97 eV (SDCI) and 2.09 eV (MCPF and CPF) and bond distances of 1.743 and 1.746 Å, respectively. These authors later report a best estimate for D_0 of 2.13 eV after correcting for basis set incompleteness,[41] in good agreement with experiment. Balasubramanian obtained similar bond lengths and BDEs of 2.09 (MCPF) to 2.19 (SOCI with Davidson's correction).[42] Our calculations find that the MoH ($^6\Sigma^+$) ground state has a BDE ranging from 2.33 eV (QCISD(T)/HW*) to 2.48 (B3LYP/HW*) eV, somewhat above the experimental value, and a bond length of 1.721 Å. An excited $^4\Phi$ ($\sigma_b^2\pi^3\delta^1\sigma^1$) state was also located lying 2.1−2.4 eV higher in energy.

Accuracy of Thermochemical Values. In assessing the accuracy of the bond energies determined in this work and our previous investigation of the $Mo^+ + CH_4$ reaction,[36] it is useful to compare the bond energies determined here both to theory and to other related metal species. Figure 4 shows the present bond energies for $Mo^+-C_xH_y$ species where $x = 0$ and $y = 1$, $x = 1$ and $y = 0-3$, $x = 2$ and $y = 1-5$, and $x = 3$ and $y = 2$ and 4. These values are compared to similar values, when available, for the same complexes but where the metal ion is Nb^+ (the neighboring element)[30] or Cr^+ (the first-row congener of Mo^+).[74,80,81] When compared to the bond energies for Nb^+, the Mo^+ BDEs are found to correlate nicely for L = H, C, CH, CH_2, CH_3, C_2H, C_2H_3, C_2H_5, and C_3H_2 with a slope such that the niobium values exceed the molybdenum values by 20 ± 13%. In contrast, the BDEs for Mo^+ binding C_2H_2 and C_2H_4 are much smaller than expected on the basis of the correlation for the other ligands. This is evidence that neither of these molybdenum bond energies correspond to the thermodynamic values, as concluded above as well.

A similar correlation is found between most of the bond energies of Mo^+-L and Cr^+-L complexes, where L includes H, CH, CH_2, CH_3, C_2H_5, and C_3H_4. The slope of this correlation indicates that chromium BDEs are smaller than the molybdenum BDEs by 37 ± 6%. Again, the BDEs between Mo^+ and L =

(79) Rayner, D. M.; Mitchell, S. A.; Bourne, O. L.; Hackett, P. A. *J. Opt. Soc. Am. B* **1987**, *4*, 900.
(80) Georgiadis, R.; Armentrout, P. B. *Int. J. Mass Spectrom. Ion Processes* **1989**, *89*, 227.
(81) Fisher, E. R.; Armentrout, P. B. *J. Am. Chem. Soc.* **1992**, *114*, 2039.

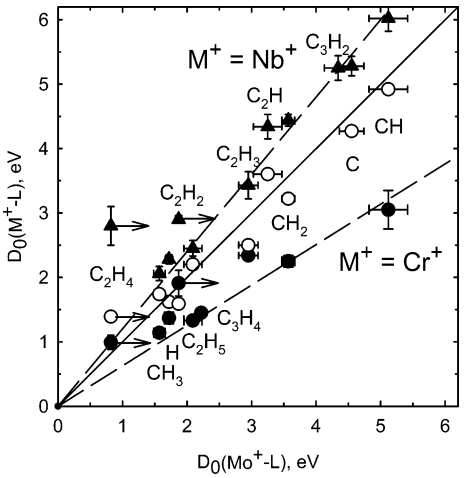

Figure 4. Comparison of experimental Mo^+-L bond energies with theoretical values (open circles) calculated at the QCISD(T)/HW*/6-311++G(3df,3p)//B3LYP/HW*/6-311++G(3df,3p) level and with experimental values for Nb^+-L (solid triangles) and Cr^+-L (solid circles) (references in the text). Lines through Nb^+ and Cr^+ data are regression lines passing through the origin and excluding the C_2H_2 and C_2H_4 points. Line through theoretical data has a slope of unity. Arrows indicate lower limits for the $Mo^+-C_2H_2$ and $Mo^+-C_2H_4$ bond energies.

C_2H_2 and C_2H_4 are much smaller than expected on the basis of the correlation and actually smaller than those for Cr^+. Although it is tempting to use these correlations to predict bond energies for the molybdenum cation alkene and alkyne bond energies, differences in the acceptor orbital available on Nb^+ versus Mo^+ and differences in the ability to sd hybridize on Cr^+ versus Mo^+ may limit the accuracy of such predictions. The other notable difference between Mo^+-L and Cr^+-L occurs for $L = C_2H_3$, which could be the result of distinct structures for these two species, although $CrC_2H_3^+$ has not been theoretically investigated.

Figure 4 also shows the comparison of our experimental Mo^+-L BDEs with those obtained from theory, specifically the QCISD(T)/HW* results. In general, there is relatively good agreement between theory and experiment with the notable exception of C_2H_4. Again, our experimental value for $D_0(Mo^+-C_2H_4)$ is too low as compared to theory, which predicts a value of 1.39 eV. In contrast, the experimental and theoretical values for $D_0(Mo^+-C_2H_2)$ are in relatively good agreement (indeed, the experimental value is above the theoretical values), in contrast to our conclusion from the correlations. These results may be an indication that the bond between the metal ion and the ligand π-bonds is not accurately described at these levels of theory.

Reactivity Differences between Mo^+ and Cr^+

The kinetic energy dependences of the reactions of Cr^+ (the first-row transition-metal congener of Mo^+) with C_2H_6 and C_3H_8 have been studied previously.[80−82] The differences in the reactivity of Cr^+ and Mo^+ can be summarized fairly succinctly. First, the efficiency of the dehydrogenation processes differs dramatically between the two metals. Although reactions 11 and 26 + 28 are endothermic and not particularly efficient, the corresponding reactions in the Cr^+ systems are not observed at any energy. Second, elimination of methane from propane, reaction 22, is endothermic and inefficient for Mo^+, whereas for Cr^+, this process is again not observed. Third, subsequent dehydrogenation of primary products (forming species such as MoC^+, $MoCH^+$, MoC_2H^+, $MoC_2H_2^+$, $MoC_2H_3^+$, $MoC_3H_2^+$, and $MoC_3H_4^+$) is pronounced in the molybdenum systems. Analogous processes in the chromium systems are generally not observed because the primary product is not formed, but in those few cases (MCH^+ and $MC_2H_3^+$) where secondary dehydrogenation is observed, these subsequent reactions are much less efficient.

Most of these differences in reactivity can be understood simply on the basis of differences in thermochemistry. As shown in Figure 4, the bond energies of chromium cations bound to H, CH_3, C_2H_5, C_3H_4, C_2H_3, CH_2, and CH (1.37 ± 0.09, 1.14 ± 0.07, 1.33 ± 0.05, 1.45 ± 0.07, 2.34 ± 0.06, 2.25 ± 0.04, and 3.05 ± 0.30 eV, respectively[11]) are approximately two-thirds the strength of those bound to molybdenum cations (Table 1). Similar results should probably hold for most other ligands. Thus, the formation of all products but MH^+ and $M(alkyl)^+$ are energetically more favorable in the molybdenum system by 1 eV or more. This clearly explains the third difference noted previously, the relative efficiency of the subsequent dehydrogenation processes. To a large extent, these energy differences also explain the first and second points, the differences in the primary dehydrogenation, and the methane elimination channels. Overall, dehydrogenation and demethanation of alkanes by Cr^+ is energetically more costly than when induced by Mo^+, but in addition, the intermediates necessary for these reactions are higher in energy. This difference in energetics is exacerbated by the relative energies of the lowest-lying quartet states of the two atomic ions. For Mo^+, ^4G ($4d^5$) has an excitation energy of 1.91 eV,[83] as compared to the ^4D ($4s^13d^4$) state of Cr^+, which lies 2.42 eV above the ground state.[84] A final consideration, as shown explicitly for the Mo^+ systems in the following paper,[71] is that these reactions require coupling between the sextet surfaces of the reactants and the quartet surfaces of the intermediates. Because of the differences in thermochemistry, these curve crossings must occur at higher energies for the chromium systems, where the coupling will be less efficient. In addition, the spin−orbit coupling necessary to mix the sextet and quartet surfaces should be more effective for the heavier metal.

Conclusion

Ground state Mo^+ ions are found to be unreactive with C_2H_6 and C_3H_8 at thermal energies, in contrast to the conclusions of Schilling and Beauchamp.[1] Thus, like Cr^+ in the first row, Mo^+ is one of the least active second-row transition-metal ions and for a comparable reason, namely, the stability of the high spin half-filled d shell configuration. Nevertheless, in agreement with Schilling and Beauchamp, Mo^+ is indeed more reactive than its first-row congener. This can be attributed to much stronger metal−ligand bonds for the second-row metal ion and to more efficient coupling between surfaces of different spins. Stronger bonds for Mo^+ can be rationalized on the basis of better hybridization of s and d orbitals, coupled with the lower excitation energy to the quartet electronic state as compared to Cr^+. The heavier metal effects dehydrogenation of ethane and propane at low energies, as well as methane elimination from propane, whereas these reactions are not observed for Cr^+ even at elevated energies.[80−82] An interesting observation in the

(82) Fisher, E. R.; Armentrout, P. B. *J. Am. Chem. Soc.* **1992**, *114*, 2049.

(83) Moore, C. E. *Atomic Energy Levels*; National Standards Reference Data Series, National Bureau of Standards (NSRDS-NBS) 35: Washington, DC, 1971; Vol. 2.

(84) Sugar, J.; Corliss, C. *J. Phys. Chem. Ref. Data* **1985**, *14*, 1.

present system is the formation of the MoH_2^+ species, which must correspond to the electrostatically bound dihydrogen complex. Similar to Cr^+, at high energies, the dominant process in the ethane and propane systems is C−H bond cleavage to form $MoH^+ + R$, although there are also appreciable contributions from $MoCH_3^+$ and $MoC_2H_5^+$ and products that result from dehydrogenation of these primary products, $MoCH^+$ and $MoC_2H_3^+$.

The endothermic reaction cross-sections observed in the systems studied here are modeled to yield 0 K bond dissociation energies for many Mo−ligand cations, as summarized in Table 1. Reasonable agreement is found for these values as compared to previous experimental and theoretical work. Complementary theoretical work allows us to identify the structures of all the product species investigated and to examine the spin states of all species as well. The thermochemistry calculated here is generally in good agreement with the experimental results. These results also make it clear that thresholds obtained for the formation of $Mo^+-C_2H_4$ and $Mo^+-C_3H_6$ must correspond to barriers to their formation. The situation is less clear for the formation of $Mo^+-C_2H_2$, although it too appears to involve a barrier to its formation. These possibilities are discussed further in the following paper.[71]

Acknowledgment. This research is supported by the National Science Foundation, Grant CHE-0451477. Dr. M. R. Sievers is thanked for acquiring all of the experimental data.

Supporting Information Available: Theoretical energies and ZPE of reactants and products calculated at several levels of theory (Table S1). Energies and structures of reactant and product ground and excited states calculated at the B3LYP/HW/6-311++G(3df,-3p) level of theory (Tables S2 and S3). This material is available free of charge via the Internet at http://pubs.acs.org.

OM700579M